

Electrochemical Detection of 4-p-nitrophenol Based on TiO₂NPs / RGO / AuNPs Composite Modified Glassy Carbon Electrode

Yongqiang Cheng, Linna Jiu, Kai Zhuo, Zhongyun Yuan, Qiang Zhang and Shengbo Sang*

MicroNano System Research Center, Key Lab of Advanced Transducers and Intelligent Control System of the Ministry of Education & College of Information and Computer, Taiyuan University of Technology, Taiyuan 030024, China

*E-mail: sunboa-sang@tyut.edu.cn

Received: 2 June 2018 / Accepted: 4 July 2018 / Published: 5 August 2018

A glassy carbon electrode modified with TiO₂NPs/RGO/AuNPs was used as an electrochemical sensor to detect trace amounts of 4-p-nitrophenol (4-NP). The surface morphology of the composites was characterized by field-emission scanning electron microscopy (FE-SEM). The electrochemical characteristics of the composite electrode were analyzed by cyclic voltammetry (CV) and electrochemical impedance spectroscopy (EIS). The modified electrode exhibited outstanding electrochemical performance due to the large specific surface area and strong conductivity of composite material. The differential pulse voltammetry (DPV) and square wave voltammetry (SWV) were used for the trace detection of p-nitrophenol. The peak current of the two methods showed a high linear relationship with the 4-NP concentration. The detection range applied DPV method was 0.5-100 μmol/L, the detection limit was 0.03 μmol/L. When SWV was employed, detection range was from 0.5 to 100 μmol/L, The detection limit was 0.08 μmol/L. In this study, the electrochemical sensor had the advantage of large detection range, low detection limit, stable, simple and fast analysis. Based on these characteristics, the sensor can be considered as a potential sensor for the detection of 4-NP.

Keywords: TiO₂NPs, RGO, AuNPs, 4-NP, Differential Pulse Voltammetry, Square Wave Voltammetry

1. INTRODUCTION

Phenol pollution in the environment mainly refers to the pollution of water by phenolic compounds. Phenol-containing wastewater is one of the most hazardous and polluting industrial wastes in the world, also is an important source of water pollution in the environment [1,2]. 4-NP is a kind of Phenol which is the most toxic among phenolic compounds. Low concentration of 4-NP cause chronic

accumulation of poisoning, high concentrations cause acute poisoning, resulting in coma or death[3]. Therefore, the United Nations, the International Maritime Organization and the United States set the 4-NP as a toxic pollutant [4], and made regulatory requirements and allowable limits on the atmosphere, surface water, water discharge, waste, food packaging and marine transportation[5-6]. The German air emission standards for nitrophenols are 20 mg/m³ (first grade), 150 mg/m³ (second grade), and 300 mg/m³ (third grade). In addition, 4-NP is widely used in chemical and organic synthesis industries, plastics, pharmaceuticals, and so on. If untreated wastewater is directly discharged to irrigate farmland, it is faced with polluting the atmosphere, water, soil and foodstuffs, posing a great threat to the environment and human health [7-8]. In general, the effective detection of 4-NP is very important.

Currently, the common detection methods for 4-NP include gas chromatography [9], liquid chromatography [10-11], UV spectrophotometry [12-13], and fluorescence spectrometry [14]. As the earliest adopted method, spectrophotometric method presented high detection limit. There are also many problems with the determination of 4-NP by chromatography, such as cumbersome operation, expensive instruments and high cost[15-20]. Comparing with above methods, the electrochemical method has expressed the advantages of convenient operation, low cost and short analysis time[21-22]. Hence, electrochemical detection has attracted a lot of attention in recent years.

Titanium dioxide, as semiconductor which can readily obtain redox-generating electron-hole pairs, have been widely applied in photovoltaics cells, photocatalytic sensors[23-26]. Additionally, TiO₂NPs-based materials are also applied in fields of electrochemical transducers and biomedicine owing to their high chemical stability, non-toxicity, high specific surface area and have a good catalytic degradation of organic compounds such as phenols and pesticides, the xu team took advantage of these properties of TiO₂NPs and used it for sensor preparation to detect dopamine and tryptophan simultaneously[27-29]. However, the activity of the catalyst TiO₂ will be reduced due to the aggregation of nanoparticles to limit the rapid electron-hole pair recombination[30]. The reduced graphene oxide is a good electrochemical sensing material, with a large specific surface area and a high electron transfer rate[31-33]. Wiench and his colleagues directly applied RGO to the surface of a glassy carbon electrode to detect 4-NP, and obtained a linear response range in 50-800μM with a detection limit is 42[34]. Studies have shown that the loading of specific nanoparticles on graphene has good photoelectrocatalytic effects on toxic organics[35]. Gold nanoparticles can improve the conductivity of the composite due to their high conductivity, distinguished biocompatibility and dispersibility[36-38]. Therefore, we designed the glassy carbon electrode modified with TiO₂NPs/RGO/AuNPs to detect the 4-NP.

2. EXPERIMENT

2.1 Instruments and reagents

ZAHNER-PP211 electrochemical workstation (Zahner, Germany); field emission scanning electron microscopy (FE-SEM, Japan, Hitachi); SFX550 ultrasonic crusher(Branson, America).

Graphene powder (50μm, Shanghai Carbon Co., Ltd.), Na₃C₆H₅O₇•2H₂O, C₇₆H₅₂O₄₆, HAuCl₄, 4-NP, NaNO₃, HNO₃, C₂H₆O(alcohol), Al₂O₃ powders(0.05μm and 0.3μm). All reagents were the

analytical grade. $[\text{Fe}(\text{CN})_6]^{3-/4-}$ solution (0.01 mol/L) was prepared with KCl, $\text{K}_4[\text{Fe}(\text{CN})_6] \cdot 3\text{H}_2\text{O}$ and $\text{K}_3[\text{Fe}(\text{CN})_6]$. And PBS buffer solution (0.067 mol/L, pH = 6.0) was formulated with NaH_2PO_4 and Na_2HPO_4 .

2.2 Preparation of $\text{TiO}_2\text{NPs}/\text{RGO}/\text{AuNPs}$ nanocomposites

Fabrication of AuNPs: Solution A was prepared including 4 ml of 0.01 g/mL $\text{Na}_3\text{C}_6\text{H}_5\text{O}_7 \cdot 2\text{H}_2\text{O}$ aqueous solution, 20 ml of deionized water, 0.5 ml 0.01 g/mL $\text{C}_{76}\text{H}_{52}\text{O}_{46}$ aqueous solution. Solution B consisted of 20 ml DI-water and 2 ml 0.01 g/mL HAuCl_4 solution. Put solution A into solution B and stirred again to combine the mixture. The color of mixed solution became purple that mean gold nanoparticles were produced.

The preparation of RGO was mainly achieved by the modified Hummers method. The fabrication of $\text{TiO}_2\text{NPs}/\text{RGO}/\text{AuNPs}$ was carried out as follow processes: 10 ml TiO_2NPs dispersion (1 mmol/L) and 10 ml AuNPs dispersion (0.5 mmol/L) were mixed together. 10 ml RGO dispersion (0.5 mg/ml) was sonicated for 20 minutes to prevent agglomeration. Then the dispersed RGO was transferred into $\text{TiO}_2\text{NPs}/\text{AuNPs}$ solution. The mixed solution was stirred at room temperature for 10 minutes to obtain a well-dispersed solution. The dispersion solution was finally centrifuged at 2000 rpm. As-prepared compounds were adjusted to 1 mL dispersion for next experiment.

2.3 Preparation of modified electrodes

The glassy carbon electrode was polished using 0.3 μm and 0.05 μm Al_2O_3 nanoparticles in sequence. Then the electrode was washed with dilute HNO_3 solution, ethanol and deionized water in turn in an ultrasonic cleaner. The cleaned electrode was naturally dry to get bare glassy carbon electrode. To prepare the modified electrode, 5 μL solution of $\text{TiO}_2\text{NPs}/\text{RGO}/\text{AuNPs}$ nanocomposite was dropped onto the bare glassy carbon electrode and naturally dried.

2.4 Analytical procedure

The experiment adopted three-electrode system: platinum mesh, Ag/AgCl and glassy carbon were used as counter electrode, reference electrode and working electrode, respectively. The electrochemical characteristics of the composite electrode were analyzed by CV (the scan range is -0.8 to 1 V, scan rate 50 mV/s) and EIS (frequency range: 0.1-10⁵ kHz) in the solution of 0.01 M $[\text{Fe}(\text{CN})_6]^{3-/4-}$ + 0.1 M KCl. The electrocatalytic properties were performed in 0.067 M PBS solution (pH = 6) containing 100 $\mu\text{mol/L}$ 4-NP with a scan rate is 50 mV/s, the scan range is -0.6 to 1.2 V. For the 4-NP detection, the DPV method is used in PBS solution with different concentrations of 4-NP (scan range: -0.6 ~ 1.2 V. Pulse period: 200 ms; Width: 50 ms; Amplitude: 20 mV; Increment: 5 mA; Scan rate: 50 mV/s). All experiments were carried at room temperature.

3. RESULTS AND DISCUSSION

3.1 Characterization of RGO and TiO₂NPs/RGO/AuNPs Composites

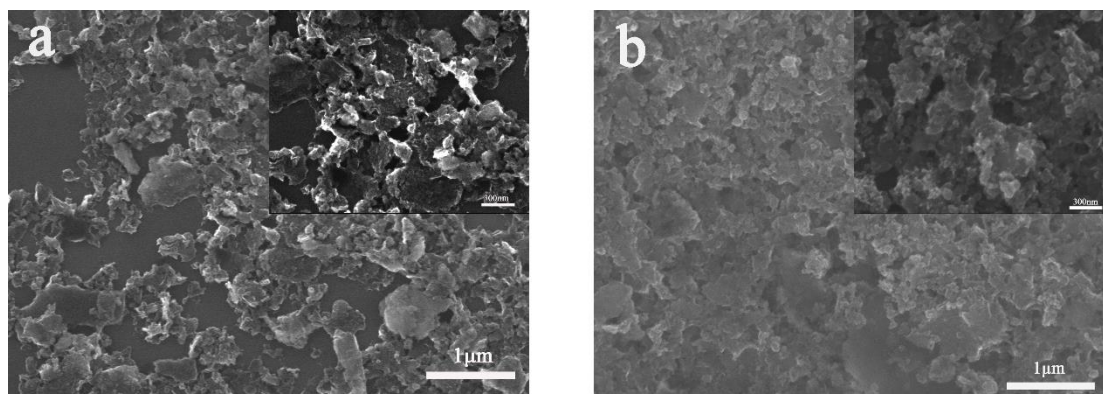


Figure 1. (a) SEM image of the RGO, (b) SEM image of the TiO₂NPs/RGO/AuNPs.

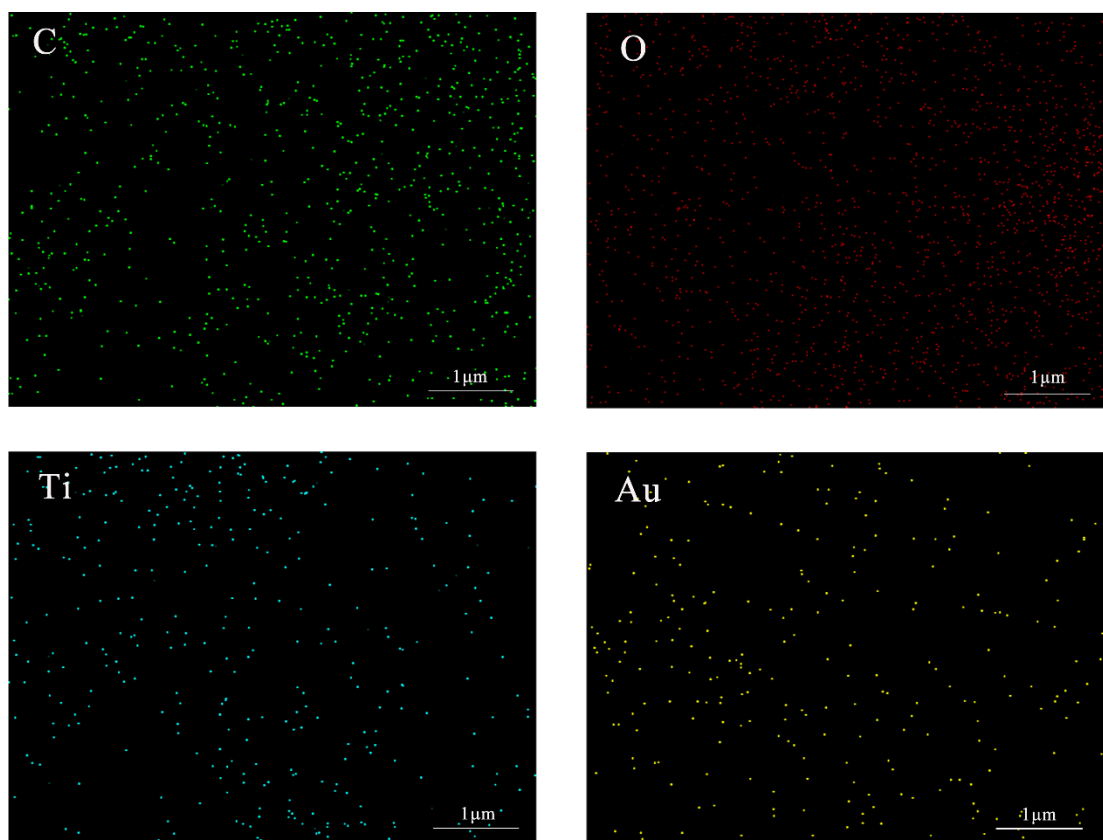


Figure 2. element distribution in the SEM surface scan.

Figure 1 (a) shows a scanning electron micrograph of the surface of RGO. RGO is a sheet-like structure with wrinkles on the surface, which increase the contact area of RGO. Figure 1 (b) shows a scanning electron micrograph of TiO₂NPs/RGO/AuNPs. AuNPs and TiO₂NPs were agglutinated on the surface of RGO. It is indicated that two kinds of nanoparticles have attached to the surface of RGO. Nanoparticles prevented the aggregation of RGO for increasing the specific surface area of composition.

Figure 2 is the elemental distribution. Three elements C, Ti, Au were evenly distributed that TiO₂NPs, AuNPs, RGO were uniformly mixed together.

3.2 Modified electrode electrochemical characterization

The modified electrode was characterized by cyclic voltammetry. The results were shown in Fig.3(a). A pair of well-defined redox peaks with a peak potential difference (ΔE) of 0.28 V appeared for bare glassy carbon electrode. The peak current of TiO₂NPs/GCE decreased comparing to the value of bare glassy carbon because of the low conductivity of TiO₂. It was considered that TiO₂ reduced the electron transfer speed between electrode inside and the electrode surface. The peak current of TiO₂NPs/RGO/GCE was obviously increased even lower than glassy carbon. The RGO enhanced the conductivity of the electrode. The redox current of TiO₂NPs/RGO/AuNPs/GCE significantly increased (curve d) and the peak potential difference (ΔE) was 0.139 V. The presence of a complex of gold nanoparticle, titanium dioxide and graphene on the glassy electrode effectively increased conductivity.

EIS impedance spectrum was applied to characterize the electrochemical conductivity of surface modification of the electrode. The semicircular diameter of the EIS represents the electrode surface electron transfer resistance (Ret) value. Fig.3(b) showed the EIS curves of different modified electrodes in 5 mmol/L [Fe(CN)₆]^{3-/4-} solution. It was seen that the spectrum *a* was the impedance spectrum of GCE and the value of the electron transfer resistance (Ret) is 93Ω. The spectrum *b* was the impedance spectrum of the modified TiO₂NPs. The value of the electron transfer resistance (Ret) was 175Ω. The semiconductor material hindered the electron transfer electrode surface, resulting in electrochemical impedance larger. Line *c* is modified impedance spectrum of TiO₂NPs/RGO. As a carrier of TiO₂NPs, RGO has superior conductivity and thus relatively reduced resistance. From the line *d*, the Ret decreased obviously at the composite modified electrode, which is close to a straight line.

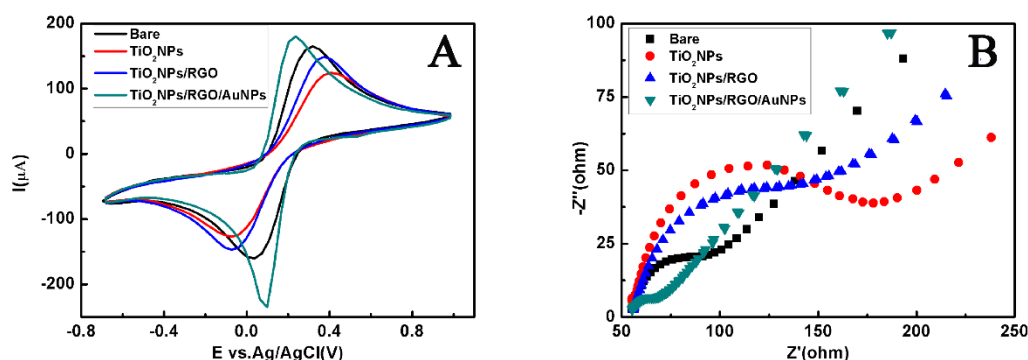


Figure 3. (A) CVs of bare GCE, TiO₂NPs/GCE, TiO₂NPs/RGO/GCE and TiO₂NPs/RGO/AuNPs/GCE in 0.01M [Fe(CN)₆]^{3-/4-} + 0.1M KCl solution. (B) Nyquist plots recorded on bare GCE, TiO₂NPs/GCE, TiO₂NPs/RGO/GCE and TiO₂NPs/RGO/AuNPs/GCE in 0.01M [Fe(CN)₆]^{3-/4-} + 0.1M KCl solution.

This phenomenon was explained that the conductive Au nanoparticles reduced the electrochemical impedance. At the same time, the change of the impedance showed that the

nanocomposite film successfully modified in the GCE. It also presented that the addition of AuNPs in the nanocomposite films improved the electron transfer rate on the composite thin film modified electrode. This was also consistent with the CV plot.

3.3 Electrocatalytic Performance of Modified Electrode

In order to investigate the effect of the modified electrode on the electrocatalytic activity of 4-NP, bare GCE, TiO₂NPs/GCE, TiO₂NPs/RGO/GCE and TiO₂NPs/RGO/AuNPs/GCE were respectively exposed to PBS solution (pH = 6) containing 100 μmol/L 4-NP. The test was carried out under scan range from -0.6 to 1.2 V with the scan rate is 50 mV/s for cyclic voltammetry. In Fig.4, no redox peaks appear on the 4-NP at GCE (a). It was demonstrated that the bare electrode has almost no electrocatalytic activity for 4-NP. TiO₂NPs/GCE expressed certain electrocatalytic activity toward 4-NP caused by mild peaks appeared. There are three obvious oxidation peaks on TiO₂NPs/RGO/GCE and TiO₂NPs/RGO/AuNPs/GCE. Both of electrodes catalyzed the 4-NP electrochemical response. Since both 4-NP and RGO contain benzene ring and similar benzene ring structure, the "π-π" effect existed between them. The adsorption effect was enhanced and the redox peak current was increased. Moreover, the TiO₂NPs/RGO/AuNPs/GCE not only contained similar benzene ring structure, the Au nanoparticles had a strong catalytic effect. At the same time, the nitro group and the hydroxyl group on 4-NP were negative in electronegativity. Electrostatic attraction force was easily generated between Au metal particles to enhance the adsorption. In addition, no significant redox peaks were observed in the CV scan of the modified electrode in the blank PBS solution, but significant redox peaks were found in the CV scan of the PBS solution with 4-NP concentration of 100 μmol/L. The redox peaks between -0.6 and 1.2 V came from the electrochemical reaction of 4-NP. As shown in Fig. 5 (A) and Fig. 5 (B), the DPV and SWV peak currents were all reached maximum value when the electrode modified with TiO₂NPs/RGO/AuNPs complex, the experiment tested in PBS solution containing 10 μmol/L 4-NP. The composition on the 4-NP catalytic performance was remarkable.

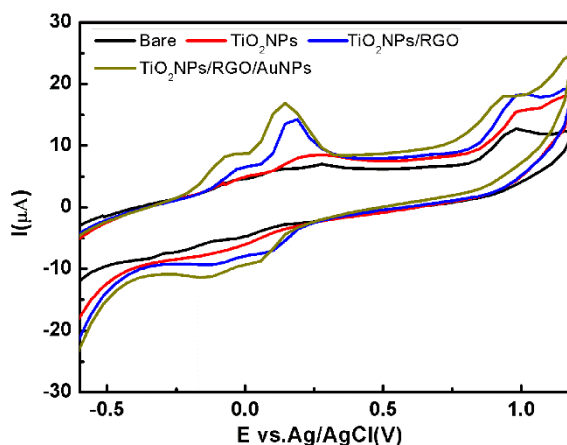


Figure 4. CVs of bare GCE, TiO₂NPs/GCE, TiO₂NPs/RGO/GCE and TiO₂NPs/RGO/AuNPs/GCE in the PBS solution (pH = 6) containing 100 μmol/L 4-NP.

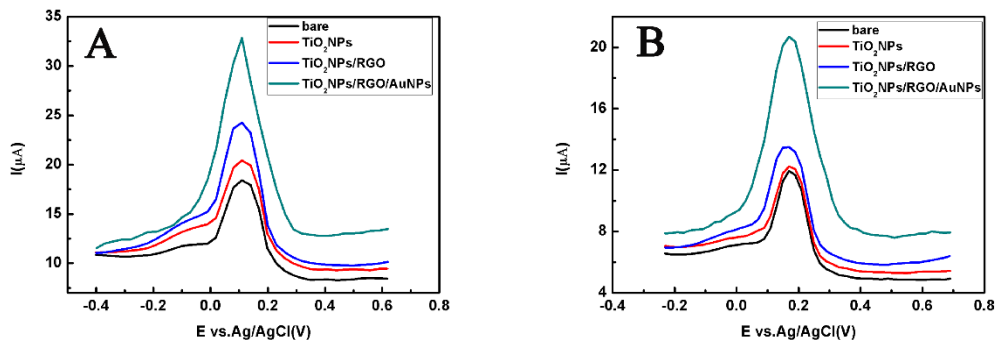


Figure 5. (A)DPV response of bare GCE, TiO₂NPs/GCE, TiO₂NPs/RGO/GCE and TiO₂NPs/RGO/AuNPs/GCE in the PBS solution (pH = 6) containing 10μmol/L 4-NP. (B) SWV response of bare GCE, TiO₂NPs/GCE, TiO₂NPs/RGO/GCE and TiO₂NPs/RGO/AuNPs/GCE in the PBS solution (pH = 6) containing 10μmol/L 4-NP.

3.4 Modified electrode DPV and SWV response to 4-NP

The 4-NP was detected by using two detection methods: SWV and DPV. Figure 6 (a) showed the DPV response of TiO₂NPs/RGO/AgNPs/GCE when the concentration of 4-NP varied from 0.5 to 100μmol/L in the PBS solution. The concentration of PBS solution was 0.067 mol/L and the pH was adjusted to 6.0. As the concentration increases, the peak current also increases and the peak current corresponds to a potential approximately at 0.16 V. The linear connection between DPV peak current and 4-p-nitrophenol concentration was shown in Figure 6 (b).

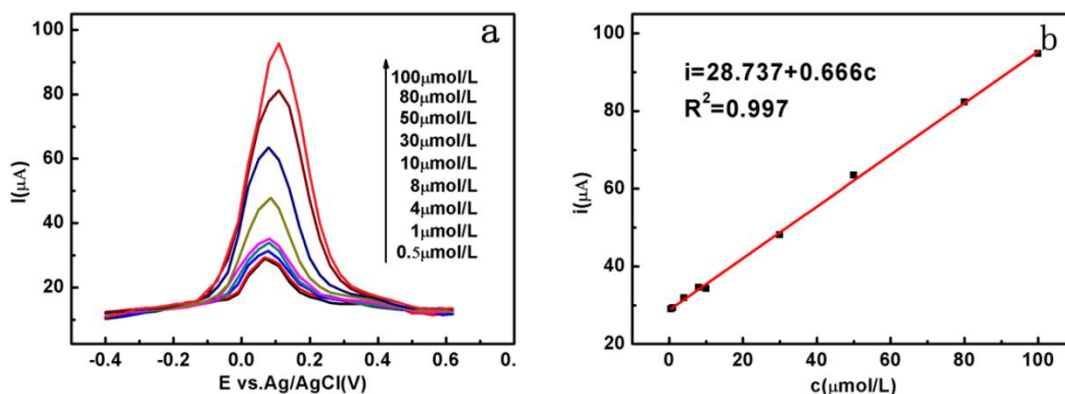


Figure 6. (a) DPV response of different concentration of 4-NP on TiO₂NPs/RGO/AuNPs/GCE in 0.067 M PBS (pH=6.0). (b) corresponding calibration.

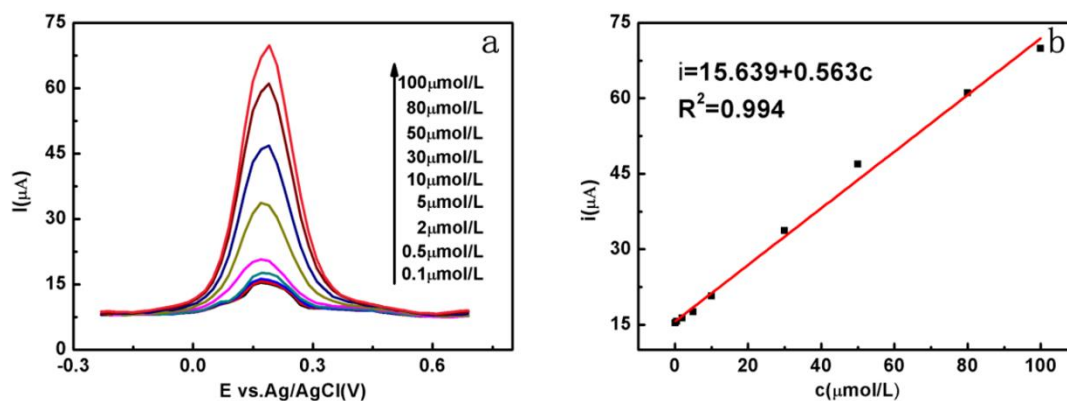


Figure 7. (a) SWV response of different concentration of 4-NP on TiO₂NPs/RGO/AuNPs/GCE in 0.067 M PBS (pH=6.0). (b) corresponding calibration.

The linear relationship was $I (\mu\text{A}) = 0.666C (\mu\text{mol/L}) + 28.737$ ($R^2=0.997$), where C represented the 4-NP concentration. The detection range was 0.5-100 μmol/L, the detection limit was 0.03 μmol/L (the detection limit was calculated as $c = \frac{3\sigma}{s}$, σ was the standard deviation of the intercept of the concentration current curve, and s was the slope of the curve). Fig. 7 (a) was the SWV response of TiO₂NPs/RGO/AuNPs modified electrode for 4-NP concentration in range 0.1 to 100 μmol/L. The experiments were carried out at a concentration of 0.067 mol/L, pH=6.0 PBS solution. Fig. 7 (b) showed that the linear connection between the peak current and the 4-p-nitropheno concentration was $I (\mu\text{A}) = 0.563C (\mu\text{mol/L}) + 15.639$ ($R^2=0.994$). The detection range was 0.1-100 μmol/L, the detection limit was 0.08 μmol/L. It was seen that the test results of these two methods were similar, the peak current and 4-NP concentration revealed a good linear connection.

Table 1 summarizes the comparison of 4-NP detection by different electrochemical sensors. TiO₂NPs /RGO/AuNPs/GCE sensor exhibited favorable detect performance for 4-NP. Metal nanoparticles have excellent conductivity, carbon materials such as graphene have large specific surface area, and there is adsorption between 4-NP, which makes the catalytic effect stronger. However, compared with Nano-gold[39] or rGO sensor[31], the TiO₂NPs /RGO/AuNPs/GCE sensor showed Lower detection limit and higher recovery, the sensor composited by AuNPs, TiO₂NPs and RGO shows an enhanced analytical performance, which is due to the synergistic effect between the materials that enhances the electrocatalytic performance of the composite to 4-NP. In addition, compared with the sensor of RGO/Fe₃O₄NPs/GCE[45], this sensor has a wider linear detection range and a lower detection limit, which is mainly due to TiO₂NPs and AuNPs have higher catalytic performance for 4-NP. Based on the advantages of high correlation coefficient, wide linear range, low detection limit and satisfactory stability, the sensor is feasible for the detection of 4-NP.

Table 1. Comparison of different electrochemical sensors performance for detection 4-NP

| Work electrodes | Linear range ($\mu\text{mol/L}$) | Detection limit ($\mu\text{mol/L}$) | Correlation Coefficient | Recovery (%) | References |
|--|------------------------------------|---------------------------------------|-------------------------|--------------|------------|
| Nano-gold/GCE | 10–1000 | 8 | ----- | 97–97.7 | 39 |
| ZnO/F/GCE | 0.035-1.4 | 0.008 | 0.9988 | 96.8-105.7 | 40 |
| | 2.1-6.3 | | 0.9977 | | |
| MWNT /GCE | 2–4000 | 0.4 | 0.9965 | 96–102 | 41 |
| AgNPs/GCE | 0.1–350 | 0.015 | ----- | ----- | 42 |
| MWNT-Nafion/GCE | 0.1–10 | 0.04 | 0.9980 | 102.6–104.6 | 43 |
| rGO-180/GCE | 50-800 | 42 | 0.9987 | 97-105 | 31 |
| SWNT/GCE | 0.01-5 | 0.025 | ----- | 98.8-104.2 | 44 |
| RGO/Fe ₃ O ₄ NPs/GCE | 0.2-10 | 0.26 | 0.9983 | 98-101.7 | 45 |
| | 20-100 | | 0.9997 | | |
| TiO ₂ NPs/RGO/AuNPs | 0.05-100 | 0.03 | 0.998 | 98-101.7 | This work |
| | 0.1-100 | 0.08 | 0.994 | 99.1-101.4 | |

3.5 4-NP test results in water samples

Table 2. Detecting recovery condition of 4-NP in water

| Added 4-NP (μM) | DPV | | SWV | |
|------------------------------|---------------------------------|--------------|---------------------------------|--------------|
| | Detected 4-NP (μM) | Recovery (%) | Detected 4-NP (μM) | Recovery (%) |
| 0.5 | 0.49 | 98 | 0.507 | 101.4 |
| 2 | 1.987 | 99.3 | 1.983 | 99.1 |
| 5 | 5.044 | 100.9 | 5.062 | 101.2 |
| 20 | 20.346 | 101.7 | 20.083 | 100.4 |
| 50 | 49.261 | 98.5 | 49.653 | 99.3 |

Adding NaH₂PO₄ and Na₂HPO₄ into the water sample to adjust pH to 6.0, no peak current was found applied DPV and SWV before adding 4-NP. When different concentrations of 4-NP were added into the water sample, the corresponding peak current appeared, the concentration values were calculated and summarized in Table 2. The sensor recovery range was 97.2-103 $\mu\text{mol/L}$ to its superior practical application.

3.6 The stability of modified electrode

The stability of glassy carbon electrode modified by TiO₂NPs/RGO/AuNPs was tested in two weeks. Figure 8 indicates there is no obvious decrease in DPV response peak current. During the 14-day storage period, the TiO₂NPs/RGO/AuNPs electrode retained 92.2% of the initial response current.

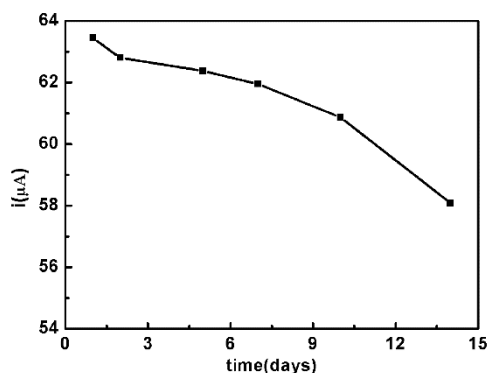


Figure 8. DPV response peak current of different storage days sensor(TiO₂NPs/RGO/AuNPs/GCE) for 4-NP's detection in 0.067 M PBS (PH=6.0).

4. CONCLUSION

In this work, TiO₂NPs/RGO/AuNPs nanocomposites were successfully prepared. The surface morphologies were characterized by FE-SEM. The electrochemical properties of the composites were characterized by CV and EIS. Using the RGO covered AuNPs and TiO₂NPs modified glassy carbon electrode, increasing the specific surface area, and fully improve the electrocatalytic properties of materials, and stability, reusable and the production. The method is simple, the cost is low, and has satisfactory application prospect.

ACKNOWLEDGEMENTS

The authors are thankful for the support by National Natural Science Foundation of China (No.61471255; No.51622507; No.61474079; No.61703298; No.51705354), Basic Research Program of Shanxi for Youths (No.201701D221110, No.2015021092), Excellent Talents Technology Innovation Program of Shanxi Province of China (201605D211023) and 863 project (2015AA042601).

References

1. P. Mulchandani, Y. Lei, W. Chen, J. Wang and A. Mulchandani, *Analytica Chimica Acta*, 470(2001)79.
2. US Environmental Protection Agency, 4-Nitrophenol, *Health and Environmental Effects Profile*. 135(1980), Washington.
3. S. Singh, N. Kumar, M. Kumar, Jyoti, A. Agarwal and B. Mizaikoff, *Chemical Engineering*

- Journal*, 313(2017)283.
4. H. Yin, Y. Zhou, S. Ai, X. Liu, L. Zhu and L. Lu, *Microchimica Acta*, 169(2010)87.
 5. J. Liu, H. Chen, Z. Lin and J.-M. Lin, *Analytical Chemistry*, 82(2010)7380.
 6. V. A. Pedrosa, L. Codognoto, S. A. S. Machado and L. A. Avaca, *Journal of Electroanalytical Chemistry*, 573(2004)11.
 7. B. Thirumalraj, C. Rajkumar, S.-M. Chen and K.-Y. Lin, *Journal of Colloid and Interface Science*, 499(2017)83.
 8. J. A. Padilla-Sánchez, P. Plaza-Bolaños, R. Romero-González, A. Garrido-Frenich and J. L. Martínez Vidal, *Journal of Chromatography A*, 1217(2010)5724.
 9. D. Hofmann, F. Hartmann and H. Herrmann, *Analytical and Bioanalytical Chemistry*, 391(2008)161.
 10. J. Karaová, J. Barek and K. Schwarzová-Pecková, *Analytical Letters*, 49(2016)66.
 11. A. Niazi and A. Yazdanipour, *Journal of Hazardous Materials*, 146(2007), 421.
 12. M. I. Toral, A. Beattie, C. Santibañez and P. Richter, *Environmental Monitoring and Assessment*, 76(2002)263.
 13. W. Zhang, C. R. Wilson and N. D. Danielson, *Talanta*, 74(2008)1400.
 14. S. Lupu, C. Lete, M. Marin, N. Totir and P. C. Balaure, *Electrochimica Acta*, 54(2009)1932.
 15. M. A. El Mhammedi, M. Achak, M. Bakasse and A. Chtaini, *Journal of Hazardous Materials*, 163(2009)323.
 16. P. R. Lima, W. de Jesus Rodrigues Santos, M. O. F. Goulart, A. A. Tanaka, S. M. C. N. Tanaka and L. T. Kubota, *Electroanalysis*, 20(2008)2333.
 17. J. Barek, H. Ebertová, V. Mejstřík and J. Zima, *Collection of Czechoslovak chemical communications*, 59(1994)1761.
 18. J. Li and W. B. Ko, *Elastomers and composites*, 51(2016)240
 19. D. Deýlová, B. Yosypchuk, V. Vyskočil and J. Barek, *Electroanalysis*, 23(2011)1548.
 20. B. Ohtani, O. O. Prieto-Mahaney, D. Li and R. Abe, *Journal of Photochemistry and Photobiology A: Chemistry*, 216(2010)179.
 21. L.F. Hanne, L.L. Kirk, S.M. Appel, A.D. Narayan and K.K. Bains, *Applied and Environmental Microbiology*, 59 (1993)3505.
 22. J. Barek, J. Cvacka, A. Muck, V. Quaiserova, J. Zima, *Electroanalysis*, 13(2001)799.
 23. T. Ohno, K. Sarukawa, K. Tokieda and M. Matsumura, *Journal of Catalysis*, 203(2001)82.
 24. K. Nagaveni, G. Sivalingam, M. S. Hegde and G. Madras, *Environmental Science & Technology*, 38(2004)1600.
 25. T. Aarthi and G. Madras, *Industrial & Engineering Chemistry Research*, 46(2007)7.
 26. M. Tian, G. Wu, B. Adams, J. Wen and A. Chen, *The Journal of Physical Chemistry C*, 112(2008)825.
 27. F. Shen, W. Que, Y. Liao and X. Yin, *Industrial & Engineering Chemistry Research*, 50(2011) 9131.
 28. C.-X. Xu, K.-J. Huang, Y. Fan, Z.-W. Wu, J. Li and T. Gan, *Materials Science and Engineering: C*, 32(2012)969.
 29. T. Tong, A. Shereef, J. Wu, C. T. T. Binh, J. J. Kelly, J.-F. Gaillard and K. A. Gray, *Environmental Science & Technology*, 47(2013)12486.
 30. J. Huang, X. Zhang, S. Liu, Q. Lin, X. He, X. Xing, W. Lian and D. Tang, *Sensors and Actuators B: Chemical*, 152(2011)292.
 31. D. Peng, J. Zhang, D. Qin, J. Chen, D. Shan and X. Lu, *Journal of Electroanalytical Chemistry*, 734(2014)1.
 32. N. J. Bell, Y. H. Ng, A. Du, H. Coster, S. C. Smith and R. Amal, *The Journal of Physical Chemistry C*, 115(2011)6004.
 33. P. Wiench, B. Grzyb, Z. González, R. Menéndez, B. Handke and G. Gryglewicz, *Journal of Electroanalytical Chemistry*, 787(2017)80.

34. Y. Zeng, Y. Zhou, T. Zhou and G. Shi, *Electrochimica Acta*, 130(2014)504.
35. Y. Tang, R. Huang, C. Liu, S. Yang, Z. Lu and S. Luo, *Analytical Methods*, 5(2013)5508.
36. H. Yin, Y. Zhou, S. Ai, X. Liu, L. Zhu and L. Lu, *Microchimica Acta*, 169(2010)87.
37. J. Li, C. Liu and Y. Liu, *Journal of Materials Chemistry*, 22(2012)8426.
38. J. Geng, H. T. Jung, *The Journal of Physical Chemistry C*, 114(2010)8227.
39. L. Chu, L. Han and X. Zhang, *Journal of Applied Electrochemistry*, 41(2011)687.
40. R. Bashami, A. Hameed, M. Aslam, I. M. Ismail and M. T. Soomro, *Analytical Methods*, 7(2015)1794.
41. C. Yang, *Microchimica Acta*, 148(2004)87.
42. C. Karuppiah, S. Palanisamy, S.-M. Chen, R. Emmanuel, M. A. Ali, P. Muthukrishnan, P. Prakash and F. M. A. Al-Hemaid, *Journal of Solid State Electrochemistry*, 18(2014)1847.
43. W. Huang, C. Yang and S. Zhang, *Analytical and Bioanalytical Chemistry*, 375(2003)703.
44. C. Yang, *Microchimica Acta*, 148(2004)87.
45. Y. Cheng, Y. Li, D. Li, B. Zhang, R. Hao and S. Sang, *International Journal of Electrochemical Science*, 12(2017)7754.

© 2018 The Authors. Published by ESG (www.electrochemsci.org). This article is an open access article distributed under the terms and conditions of the Creative Commons Attribution license (<http://creativecommons.org/licenses/by/4.0/>).